MOLECULAR AND CELLULAR BIOLOGY, Aug. 1993, p. 5070–5084
0270-7306/93/085070-15$02.00/0

Vol. 13, No. 8

Alteration of a Yeast SH3 Protein Leads to Conditional Viability with Defects in Cytoskeletal and Budding Patterns

FLORIAN BAUER, MARIA URDACI,† MICHEL AIGLE, AND MARC CROUZET*

Laboratoire de Génétique, Centre National de la Recherche Scientifique Unité Recherche Associée 542, Avenue des Facultés, Université de Bordeaux II, 33405 Talence Cedex, France

Received 28 January 1993/Returned for modification 17 March 1993/Accepted 24 May 1993

Mutations in genes necessary for survival in stationary phase were isolated to understand the ability of wild-type *Saccharomyces cerevisiae* to remain viable during prolonged periods of nutritional deprivation. Here we report results concerning one of these mutants, *rvs167*, which shows reduced viability and abnormal cell morphology upon carbon and nitrogen starvation. The mutant exhibits the same response when cells are grown in high salt concentrations and other unfavorable growth conditions. The *RVS167* gene product displays significant homology with the Rvs161 protein and contains a SH3 domain at the C-terminal end. Abnormal actin distribution is associated with the mutant phenotype. In addition, while the budding pattern of haploid strains remains axial in standard growth conditions, the budding pattern of diploid mutant strains is random. The gene *RVS167* therefore could be implicated in cytoskeletal reorganization in response to environmental stresses and could act in the budding site selection mechanism.

In *Saccharomyces cerevisiae*, nutrient availability coordinates cell growth and proliferation. In medium containing all essential growth elements, yeast cells proliferate and cell growth and division are held in balance by the necessity of a minimum cell size before beginning a new division cycle (36). If one of the essential elements, for example, carbon or nitrogen, becomes exhausted, yeast cells stop division in the nonbudding G_1 phase of the cell cycle (81). The culture then is in stationary phase, and cells can remain in the living state for prolonged periods under conditions which are not propitious for growth. Indeed, in their natural environment, yeast cells spend only a small fraction of their existence in exponential growth, because of the limited availability of nutriments.

The transition from exponentially growing cells to arrested stationary-phase cells following nutrient starvation is accompanied by a number of molecular and physiological changes. At the molecular level, accumulation of glycogen and trehalose (48) is observed. The global analysis of proteins synthesized under starvation conditions reveals a subset of proteins whose synthesis increases in nutritional deprivation (9, 32). In addition, synthesis of most of the proteins expressed during exponential phase ceases (9). Physiological changes concern a higher resistance to heat shock (60), to lytic enzymes (20), and to a large number of other environmental stresses.

There are mainly two questions related to stationary-phase entry. The first question concerns the mechanisms implied in cell proliferation control in response to the nutrient starvation. Some of the molecular regulatory elements of cell proliferation control are now relatively well-known in *S. cerevisiae*. Thus a multitude of observations has been taken as evidence that the cyclic AMP (cAMP) pathway could be a signal-transmitting pathway for growth arrest following nutrient exhaustion (35, 50, 77). But it is clear that this mechanism is not the only signal-transmitting pathway responding to the nutritional environment. Genetic evidence for the existence of at least one cAMP-independent proliferation control system acting in response to nutrient starvation has been demonstrated (11). However, very little information exists about the molecular mechanism involved. A possible candidate for a cAMP-independent control pathway is the cyclin-mediated mitotic control system. This mechanism is thought to regulate cell cycle progression and division in *S. cerevisiae* and other organisms via the $p34^{CDC28}$/cyclin complex (45, 72).

The second question about stationary-phase entry concerns the comprehension of the molecular and physiological machinery of cell adaptation to starvation. Indeed, no direct relation between the physiological aspects of stationary-phase cells and concomitant molecular events has been established. Further questions are raised by the obvious, but not yet identified, links between the proliferation control mechanisms and the molecular and physiological adaptations of stationary-phase cells.

For a better understanding of the setup of the resting state and long-term cellular survival in *S. cerevisiae*, we have selected mutant strains showing loss of viability after depletion of essential nutrients, i.e., incapacity to enter stationary phase properly. The main criteria used for mutant selection were as follows. First, cell viability and cell growth in mutant cells during exponential phase should be identical to what is observed for wild-type cells. Second, the cell viability in nutrient-depleted medium should be significantly reduced. This alteration should be observed for different types of nutrient starvation in order to exclude mutants showing a specific response linked only to an essential element. Mutants showing the defined phenotype upon carbon and nitrogen starvation were retained. Several *rvs* (reduced viability upon starvation) mutants were selected. Two of the mutants corresponding to these criteria appeared to be particularly interesting because, in addition, they show morphological alterations and an increased budding ratio in starvation conditions, suggesting a possible relation between loss of viability and proliferation control. Several mutants showing similar phenotypes have already been isolated. In particular, mutations in genes in the cAMP pathway as $RAS2^{Val-19}$ (39)

* Corresponding author.
† Present address: Genius-Biotechnologie, Université de Limoges, 87060 Limoges Cedex, France.

TABLE 1. *S. cerevisiae* strains used in this study

Strain	Relevant genotype	Source
X2180-1A	*MAT***a**	Yeast Genetic Stock Center
X2180-1B	*MATα*	Yeast Genetic Stock Center
LG100-1A	*MAT***a** *trp1*	Our laboratory
LG16-5A	*MAT***a** *ura3*	Our laboratory
X2180-2N	*MAT***a**/*MATα*	Our laboratory
LG450-2N	*MAT***a**/*MATα trp1/trp1 rvs167-1/RVS167*	Our laboratory
LG500-2N	*MAT***a**/*MATα rvs167-1/rvs167-1*	Our laboratory
LG400-1A	*MAT***a** *rvs167-1*	Our laboratory
LG400-1B	*MATα rvs167-1*	Our laboratory
LG30-4A	*MATα rvs167-1 ura3*	Our laboratory
LG440-1A	*MAT***a** *rvs167-1 trp1*	Our laboratory
LG430-1A	*MAT***a** *rvs167::TRP1 trp1*	Our laboratory
LG510-2N	*MAT***a**/*MATα rvs167::TRP1/rvs167::TRP1 trp1/trp1*	Our laboratory
LG38-3B[a]	*MAT***a** *RAS2*$^{Val\text{-}19}$ *leu2-1*	Our laboratory
B-7589	*CHR4::URA3*$^+$ *MAT***a** [*cir*^{0}] *ura3-52 leu2-3,112 trp1-289 his3-Δ1 met2 cyh*^{R}	L. P. Wakem and F. Sherman
B-7595	*CHR12::URA3*$^+$ *MAT***a** [*cir*^{0}] *ura3-52 leu2-3,112 trp1-289 his3-Δ1 met2 cyh*^{R}	L. P. Wakem and F. Sherman

[a] Obtained by directed mutagenesis.

and *bcy1-1* (51) or in the cyclin-mediated cell cycle control as *CLN3*$^{DAF1\ WHI1}$ (16, 74) lead to strains showing high budding ratios and viability loss upon starvation. Nevertheless, they have not been selected for those criteria.

The two mutants *rvs161* (17) and *rvs167* were studied further. Here we report physiological and molecular characterization of the *rvs167* mutant. The *RVS167* gene was cloned by complementation, and the gene product contains a SH3 domain. Our investigations show that cytoskeletal actin is delocalized in *rvs167* mutants; furthermore the budding pattern is altered only in the diploid mutant strains. The results suggest that the Rvs167 protein may function by interacting with proteins involved in cytoskeletal reorganization in response to particular growth conditions and in bud site selection.

MATERIALS AND METHODS

Strains and media. The *S. cerevisiae* strains used in this study are derived from strain X2180 (Yeast Genetic Stock Center, Berkeley, Calif.). They are listed in Table 1. The *rvs* mutants were obtained after UV mutagenesis and analysis on test media. Test media limited for nitrogen (N0.05) or carbon (G1) source were described by Bonneu et al. (8). The N0.05 medium contains 2% dextrose, 0.17% yeast nitrogen base without amino acids and without ammonium sulfate (Difco), and 50 mg of ammonium sulfate per liter. The G1 medium is made of 0.1% dextrose and 0.67% yeast nitrogen base without amino acids. Erythrosin B (7.5 μM final concentration) was added in these test media to visualize the mutant phenotype on petri dishes, because mutant strains with low viability will give red colonies whereas wild-type colonies stay white (8). The yeast complete (YPD), minimal (YNB), and respiratory (YNBGE) media were made as previously described (67). Yeast cells were grown at 30°C unless otherwise indicated. Strain constructions followed standard methods for genetic crosses, sporulation, and tetrad dissection (54). Yeast growth was followed by measuring the optical density at 600 nm. One optical density unit corresponds to 2.4×10^7 haploid cells per ml for both wild-type and mutant strains. Cell viability and budding ratio were determined as described by Crouzet et al. (17).

The *Escherichia coli* strains used for cloning and plasmid propagation were MC1066 [F$^-$ *ΔlacY74 galU galK strA pyrF74* Tn*5* (Km^r) *leuB6 trpC9830 hsdR-K*], DH5α [F$^-$ *supE44 thi-1 recA1 gyrA96 relA1 hsdR17* (r_K^- m_K^+) *endA1* φ80d*lacZ*ΔM15 Δ(*lacZYA-argF*)U169], and JM101 [*supE thi recA*$^+$ r_K^+ Δ(*lac-proA,B*)/F′ *traD36 proA,B*$^+$ *lacI*^{q}ZΔM15]. *E. coli* strains were grown at 37°C on LB medium (53) supplemented with 50 μg of ampicillin per ml to select plasmid transformants.

Glycogen determination. Glycogen was measured by the method of Becker (6). Samples of culture medium were filtered on a nitrocellulose membrane (0.45-μm pore size; 47-mm diameter; Millipore). Filtered cells (40 mg [wet weight]) were stored at −80°C. Glycogen was extracted from frozen cells by a hot alkaline hydrolysis and then enzymatically cut in glucose units by α-amyloglucosidase. Resulting glucose was then measured by the enzymatic method (kit 115-A; Sigma Biochemicals). One unit of glycogen is 1 mg of glucose per g (wet weight) of *S. cerevisiae*.

Plasmids. All plasmids used were *E. coli-S. cerevisiae* shuttle vectors. The wild-type genomic library was constructed by inserting partially *Sau*3A-digested DNA at the *Bam*HI site of pUKC200 (gift of M. Tuite, University of Kent). Subcloning of the complementing plasmids pUKC200-9 and pUKC200-134 was done with the pFL38 plasmid (gift of F. Lacroute, Université de Paris VI). The wild-type *RVS167* gene was disrupted by insertion of a *Bgl*II fragment from plasmid pFL39 (gift of F. Lacroute) containing the *TRP1* gene into the *Bam*HI site of *RVS167*. Yeast cells were transformed by the LiCl method (34). Transformation of *E. coli* was done by the $CaCl_2$ method described by Okayama and Berg (58).

DNA manipulations. Restriction enzymes and other DNA modification enzymes were purchased from Boehringer Mannheim and used according to the specifications of the manufacturer. Plasmid DNA from *E. coli* was prepared by the method of Birnboim and Doly (7). Yeast plasmid and genomic DNA extractions were made by the method of Hoffmann and Winston (31). The sequence was determined by the dideoxy chain termination method (66) on single-stranded M13tg130 and M13tg131 (40) or directly on double-stranded plasmid DNA (44) by the Sequenase enzyme system (U.S. Biochemical Corp.) and ^{35}S-dATP (Amersham). RNA for transcript analysis was prepared by standard methods (52). Southern and Northern (RNA) blots were made as described previously (52, 71). DNA fragments were labeled

by [α-^{32}P]dATP and a random priming labeling kit (Boehringer Mannheim).

Sequence comparisons. Research for DNA and protein homologies was done with the GenBank, EMBL and SWISS-PROT data bases by using the FASTA program (59). Comparison of Rvs161 and Rvs167 proteins was carried out by the method of Needleman and Wunsch (56) with 100 runs with randomized sequences and using a unitary matrix (56). The same comparison was carried out with the proteins presenting the best alignment scores with Rvs167 protein after the FASTA searches in the cited data bases. Alignment of Rvs161 and Rvs167 was done by the method of Myers and Miller (55).

Actin localization. Fixed yeast cells were stained with rhodamine-phalloidin by the method described by Amatruda et al. (4). Cells were grown in liquid culture in the conditions described and fixed by the addition of formaldehyde directly to the culture to a final concentration of 3.7%. After 10 min, cells were collected by filtration and resuspended in 0.1 M KH_2PO_4, pH 7.0 (KPi)–3.7% formaldehyde. Cells were collected after 1 h, washed in KPi containing 5 mM ethanolamine, and resuspended in KPi containing 3.3 μM rhodamine-conjugated phalloidin (Sigma). After 2 h at 4°C, cells were washed four times in KPi and mounted directly for microscopic observation.

Visualization of cell wall chitin. Chitin was visualized by fluorescence microscopy after cells were stained with 0.1% calcofluor (Fluorescent Brightener 28; Sigma) for 5 min and washed four times in distilled water (62).

Generation of anti-*RVS167* antibodies. *trpE-RVS167* and *gst-RVS167* fusion proteins were produced and purified from *E. coli*. The *trpE-RVS167* fusion protein was obtained by cloning a DNA fragment, *Bam*HI-*Sph*I, of 1,510 nucleotides, containing the major part of the open reading frame of the *RVS167* gene, into the corresponding sites of plasmid pATH22 (43). The *gst-RVS167* fusion protein was obtained by cloning a *Bam*HI-*Hin*dIII DNA fragment from the multicloning site of the pFL38 plasmid containing the *RVS167* gene into the pGEX-A plasmid (70). *E. coli* HB101 strains transformed by these plasmids synthesized fusion proteins of 88 kDa for *trpE-RVS167* and 77 kDa for *gst-RVS167* upon induction. The fusion proteins were purified from the insoluble fractions by sodium dodecyl sulfate (SDS)-polyacrylamide gel electrophoresis. Two rabbits were first injected with 200 μg of *trpE-RVS167* fusion protein emulsified in Freund's complete adjuvant (Sigma). These injections were followed by booster injections of 100 μg of the *gst-RVS167* fusion protein emulsified with Freund's incomplete adjuvant (Sigma) 18, 33, and 48 days after the primary injection. The choice of a second fusion protein was made to limit cross-reactions between anti-*trpE* antibodies and yeast proteins.

Immunoblotting. Yeast proteins were prepared by rapid glass bead disruption as described by Boucherie (9). Protein samples were boiled in sample buffer containing 1% SDS and run on an SDS–10% polyacrylamide gel (46). Proteins were electroblotted to an Immobilon membrane (Millipore) for 1 h at 0.8 mA/cm^2. Membranes were blocked by incubation at 28°C and agitation (60 rpm) for 1 h in TBS buffer (50 mM Tris HCl [pH 8.5], 150 mM NaCl, 0.1% Tween 20) containing 4% bovine serum albumin (BSA). Membranes were washed 5 min in TBS buffer and then incubated in TBS buffer containing 0.1% BSA and anti-Rvs167p antiserum for 12 h at 28°C. After a new wash in TBS, membranes were incubated in TBS buffer with 1 μCi of ^{35}S-labeled protein A (Amersham)–4% BSA for 2 h. Finally, membranes were washed three times (5 min) in TBS buffer, dried, and exposed to autoradiography.

Nucleotide sequence accession number. The sequence of the *RVS167* gene has been submitted to GenBank and assigned accession number M92092.

RESULTS

Description of the *rvs167* mutant. The *rvs167* mutant was isolated among mutagenized cells giving red colonies on N0.05 and G1 media supplemented with the vital stain erythrosin B (8). The original mutant strain was backcrossed three times with the wild type. Through genetic crosses, we demonstrated that the *rvs167-1* mutation is recessive and segregates as a single gene. Further analysis was done on the LG400-1A and 1B strains issued from the last backcross. *rvs167* mutant cell growth, cell division, and viability in liquid cultures were studied in different growth conditions and for different types of starvation and compared with those of the wild type. Figure 1 shows the results obtained for carbon starvation in G1 medium under standard growth conditions. Mutant cells are indistinguishable from wild-type cells in exponentially growing cultures in respect to growth rate (Fig. 1A), budding percentage (Fig. 1B), and cell viability (Fig. 1C). No apparent difference was observed in cell size and shape. When entering stationary phase in response to carbon exhaustion, wild-type cells accumulate in the nonbudding G_1 phase. In the conditions used, the budding percentage of the wild-type strain decreases from 60% in the exponential phase of growth to 5% in stationary phase and viability is maintained. In the same conditions, a rapid decrease in survival ratio of mutant cells is observed. Twelve hours after stationary-phase entry in carbon-depleted medium, approximately 50% of cells present at entry are still able to form colonies against nearly 100% for the wild-type strain. Although obvious at stationary-phase entry, the loss of viability is not very dramatic, and 3 days after carbon exhaustion 30% of the mutant cells remain viable. Moreover, at plateau the percentage of budded cells is still high for the mutant strain. After 24 h in stationary phase, it is about 25%, compared with 4 to 5% for wild-type cells.

Microscopic observation of the *rvs167* mutant cells in starvation conditions reveals abnormal morphology, important heterogeneity in size and shape, and frequent cellular lysis (Fig. 2A). Huge swollen cells filled by large vacuoles coexist with very small cells, corresponding probably to buds separated from mother cells before having reached normal size; 15 to 20% of the cells present an abnormal morphology. All these alterations become more pronounced after a few days of starvation. The budding is not linked to one abnormal cell type, and microscopic examination using the vital stains erythrosin B and methylene blue (8) does not show any correlation between the inviable cells and the budded ones. When cells are starved for nitrogen in N0.05, the viability loss with altered morphology, although less pronounced, is also observed (data not shown). The *rvs167* mutant develops the same terminal phenotype when cells are depleted of sulfate or phosphate (data not shown). These results suggest that the mutation should affect the general response to nutritional starvation.

In these conditions the *rvs167* mutant phenotype seems specific to stationary-phase setup. At stationary-phase entry, physiological and molecular changes such as synthesis and accumulation of glycogen (48) and induction of heat shock proteins (9) have been described. Mutant cells are able

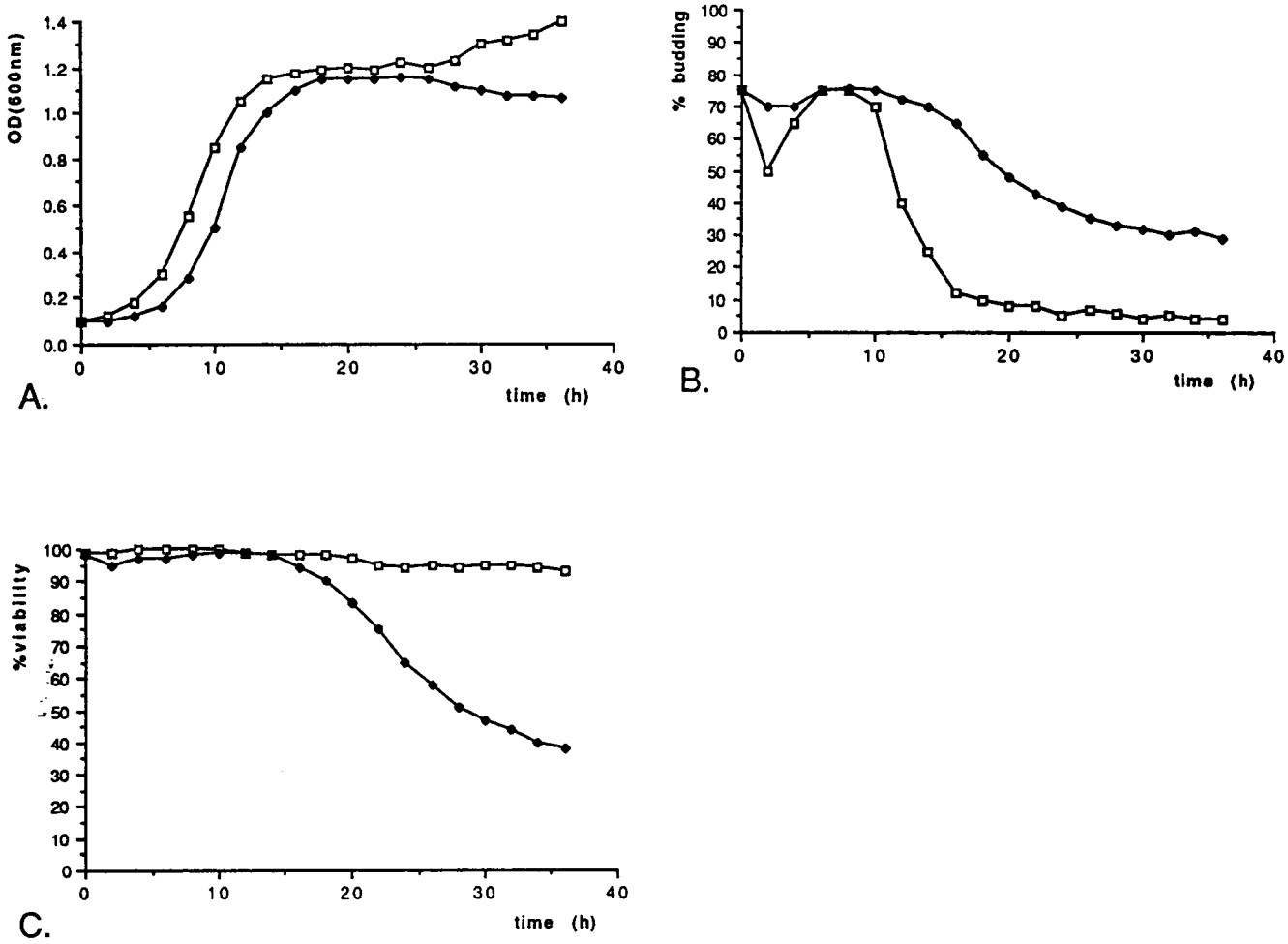

FIG. 1. Growth (A), budding percentage (B), and viability (C) of wild type (open square) and *rvs167* mutant (black circle) in carbon-limited, G1 liquid medium. Cultures were done in 100 ml at 200 rpm and at 30°C in 500-ml Erlenmeyer flasks. (A) Growth was determined by measuring the optical density at 600 nm. One optical density unit equals 2.4×10^7 cells per ml. Doubling time and stationary-phase plateau are similar for mutant and wild-type cells. (B) Budding percentage of mutant and wild-type cells was determined by microscopic examination after 10 s of mild sonication. (C) Cell viability was determined by colony counts as described in Materials and Methods.

to accumulate glycogen just before entering stationary phase in the same way as wild-type cells (Fig. 3A). On the other hand, mutant cells are slightly less resistant to heat shock when cells are exposed to a temperature of 55°C for 1 h (Fig. 3B). Growth is also slightly affected during the shift of liquid cultures from 21 to 37°C. However, the mutant is not thermosensitive for growth. The sensitivity to the high-temperature shock seems to be unrelated to the molecular heat shock response. The induction of heat shock proteins is normally regulated in the *rvs167* strain. This was shown by following the synthesis of heat shock proteins by two-dimensional electrophoresis after in vivo labeling with [^{35}S]methionine (unpublished data).

The mutant strain LG400-1A or 1B carrying the mutation *rvs167-1* exhibits other phenotypes not directly associated with stationary-phase entry (Fig. 4). The mutant proved to be unable to grow on nonfermentable carbon sources. Nevertheless, [*rho*$^-$] strains do not display the phenotype of *rvs167* cells during stationary-phase entry, indicating that these characteristics do not originate from changes in energy metabolism. The mutant growth is also altered by the addition of salt in the culture medium. In particular, the *rvs167* cells are unable to grow on medium with high salt concentrations (6% NaCl or 6% $MgCl_2$). Moreover, the mutant strain is hypersensitive to the amino acid analog canavanine and the inhibitor 3-amino-1,2,4-triazole (82). Growth of mutant cells is totally inhibited at 20 mM 3-amino-1,2,4-triazole and 1 μg of canavanine per ml, whereas wild-type growth is not affected at these concentrations. Surprisingly, although not starved, the cells show in the presence of salts (Fig. 2B) or inhibitors the same morphological alterations and viability defects already observed in starvation conditions.

Furthermore, all these pleiotropic effects of the *rvs167* mutation are also observed in another *rvs* mutant, the strain mutated for the *RVS161* gene (17). These phenotypes are not enhanced in the strain carrying both the *rvs161-1* and *rvs167-1* mutations.

Cloning and sequencing of the *RVS167* gene. The wild-type *RVS167* gene was isolated by transforming mutant LG440-1A cells with a library of yeast genomic DNA in a centromere-containing pUKC200 vector. Colonies were first screened for cell viability on erythrosine B-containing test medium as described by Bonneu et al. (8). Two transfor-

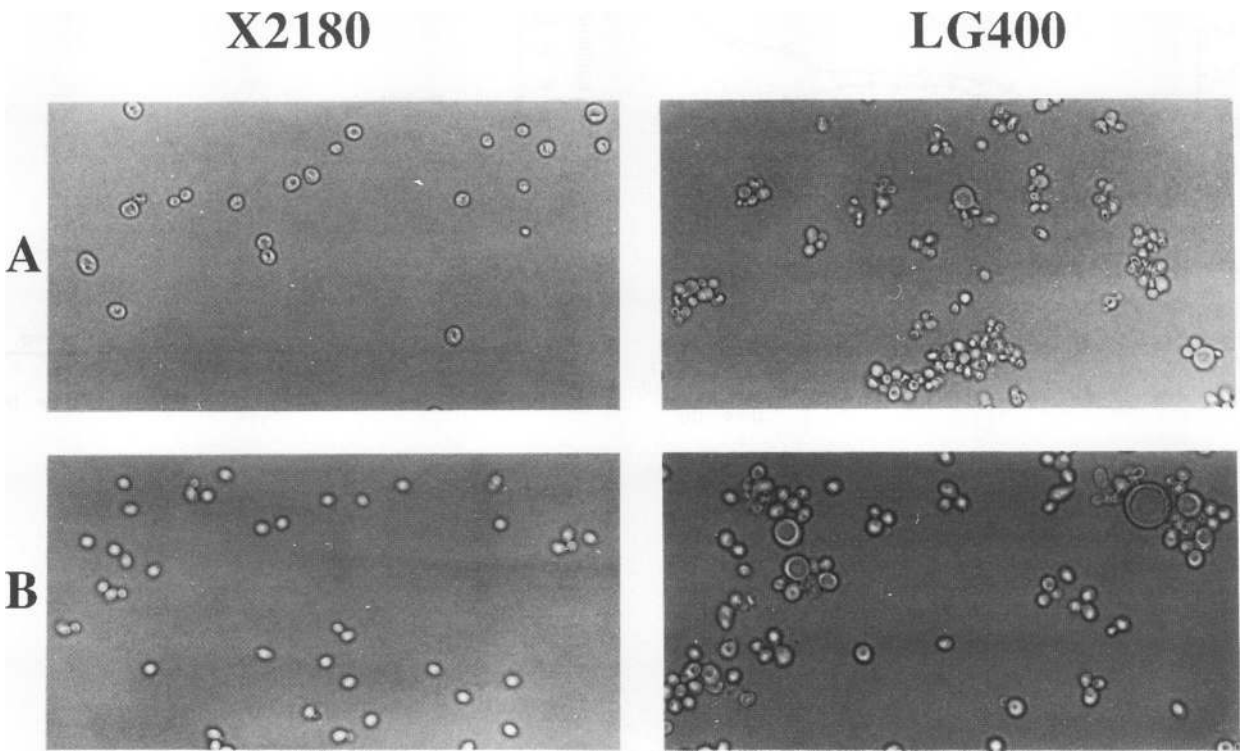

FIG. 2. Effect of the *rvs167-1* mutation on cell morphology. (A) Morphology of cells in medium G1 24 h after stationary-phase entry. (B) Effect of addition of NaCl (3%) on exponentially growing cells in YPD medium.

mants with wild-type viability were obtained and verified for complementation of all the *rvs167* characteristics described above. The two plasmids were isolated and tested for their ability to complement the *rvs167-1* mutation upon retransformation. The plasmids which present overlapping restriction maps were subcloned. The complementing activity resides on a 1.8-kb *Kpn*I-*Sph*I fragment (Fig. 5A).

This fragment and adjacent regions were sequenced. The sequence revealed a single long open reading frame of 1,446 nucleotides, coding for a putative protein of 482 amino acids (Fig. 5B). The molecular weight of the putative Rvs167 protein is estimated as 53,000, with a calculated pHi of 5.64.

Genomic DNA digested by different restriction enzymes was tested by Southern analysis with the 1.8-kb *Kpn*I-*Sph*I fragment containing the entire open reading frame. In all cases a single band responded, showing that *RVS167* is a single-copy gene (data not shown). The same *Kpn*I-*Sph*I fragment was used to probe a yeast chromosome blot. Results were ambiguous because of bad resolution of chromosomes IV and XII. The *RVS167* gene was finally localized by the method described by Falco et al. (24). A recessive mutation in a [cir$^+$] strain can be assigned to its chromosome by crossing to each of the [cir^0] tester strains containing the 2μm inverted repeat sequence and isolating the [cir$^+$]/[cir^0] diploids. The recessive mutation will only be manifested in the diploid containing the [cir^0] tester strain with an integrant in the same chromosome the mutation is on. The strain LG400-1B carrying the *rvs167-1* mutation was crossed with the chromosome tester strains B-7589 and B-7595 (P. Wakem and F. Sherman, Department of Biochemistry, University of Rochester Medical Center); the *rvs167* phenotype appeared only in diploids from crosses between the *rvs167* strain and strain B-7595, showing that *RVS167* is on chromosome XII. To verify genetic mapping, the *rvs167* strain was crossed with strains carrying different markers (*spa2*, *asp5*, *gal2*, *tfs1*, *cdc42*, *cdc25*, *ilv5*, *ura4*, *leu3*) located on chromosome XII; no linkage to these genetic markers was observed.

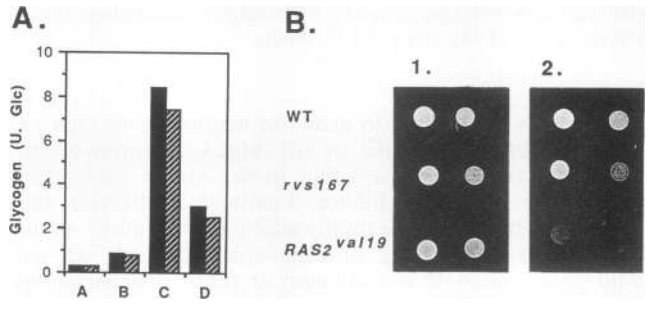

FIG. 3. (A) Glycogen accumulation at stationary-phase entry in wild-type and *rvs167* mutant strains. Black bars represent accumulation in wild-type cells; hatched bars represent accumulation in mutant cells. Strains were grown in liquid YNB medium as described in Materials and Methods. Glycogen accumulation was determined at different growth phases: A, exponential growth; B, beginning of stationary-phase entry; C, end of stationary-phase entry; D, 3 h after stationary-phase entry. One unit of glycogen (U. Glc) is 1 mg of glucose per g of yeast (wet weight). (B) Heat-shock sensitivity of *rvs167* mutant strain compared with that of the wild-type strain and the *RAS2*$^{Val-19}$ strain (LG38-3B). This last strain is known to be sensitive to heat shock. Cellular suspension (5 μl) from strains in exponential growth phase (2.5×10^4 cells for the first drop and 2.5×10^3 cells for the second drop in each line) was spotted on YPD plates. Plate 2 was immediately put for 1 h at 55°C; plate 1 was not. Afterwards, plates were incubated at 30°C for 40 h.

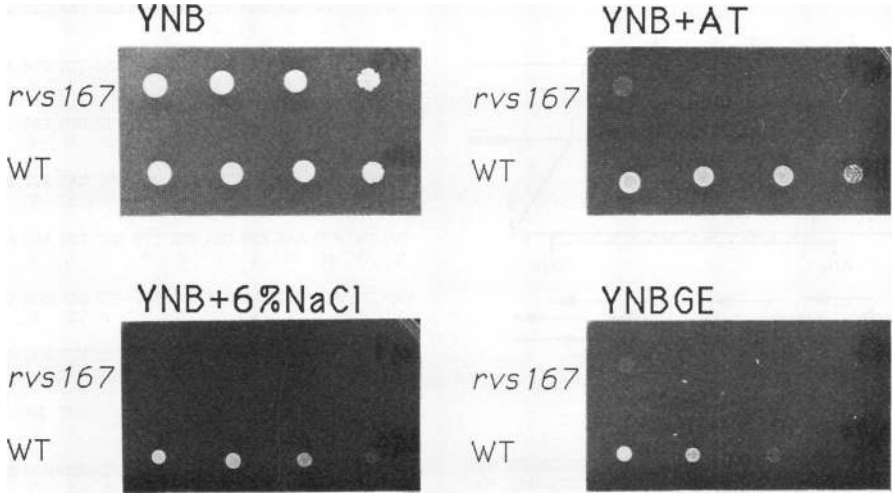

FIG. 4. Growth of wild-type and *rvs167* mutant strains in different conditions. From each strain in exponential growth phase, four drops of a cellular suspension (5 μl) containing decreasing amounts of cells were spotted on plates of YNB, YNBGE, and YNB supplemented with 20 mM 3-amino-1,2,4-triazole (AT) or 6% NaCl. The mutant strain shows normal growth on the YNB plate but was unable to grow in the other conditions tested.

Disruption of the *RVS167* gene. To ensure that the cloned gene is *RVS167* and not a suppressor of the mutation *rvs167-1*, and to determine the phenotype of the disrupted strain, we disrupted the gene by the one-step gene disruption method (64). The *TRP1* gene from vector pFL39 (gift from F. Lacroute) was inserted at the *Bam*HI site of the cloned gene. This site is situated downstream from the ATG translation start site at position +86. A diploid strain, LG450-2N (*trp1/trp1 RVS167/rvs167-1*), was transformed with the *Kpn*I-*Sph*I DNA fragment in which the *TRP1* cassette has been inserted. Approximately half of the Trp^+ colonies recovered after transformation showed the *rvs167* phenotype on erythrosin B-containing test media, suggesting that the wild-type *RVS167* allele was disrupted. Segregation analysis was performed on three Trp^+ transformants showing the wild-type phenotype. For each transformant, four viable spores were recovered in each tetrad dissected with the Mendelian segregation 2 Trp^+:2 Trp^-. All haploid Trp^+ cells present the same phenotype as the *rvs167* original mutant in regard to all the characteristics tested, while all Trp^- cells are wild type for *rvs167* characteristics. Segregation analysis of the *rvs167-1* primary mutation and the disrupted gene indicates that integration of *TRP1* took place at the *RVS167* gene locus. This finding has been confirmed by complementation analysis of the diploid strain containing the original *rvs167-1* mutation and the disrupted gene. Disruption was verified further by Southern and Northern blot analysis (data not shown). This analysis showed that the genomic gene was disrupted as expected. Furthermore, no transcript corresponding to *RVS167* was found in the disrupted cells (data not shown). The cloned gene, therefore, is the *RVS167* gene. The gene *RVS167* is not an essential gene, and the strain LG430-1A carrying the *rvs167::TRP1* null allele presents the same phenotype as the *rvs167* original mutant.

Northern and Western analysis. Northern analysis (Fig. 6A) revealed a transcript of about 1.65 kb which is present in exponentially growing cultures and disappears during stationary phase. This transcript exists in the *rvs167* mutant strain. The level of transcription seems not to be significantly altered by heat shock and by growth on nonfermentable carbon sources.

Western analysis of total protein extract revealed a protein with an apparent molecular weight of 57,000, compatible with the expected weight of 53,000. This protein is absent in disrupted cells, as in the original mutant (Fig. 6B), and therefore it is the *RVS167* gene product. The protein is present mainly in exponentially growing cultures and disappears in late stationary phase (data not shown).

Sequence analysis. Nucleotide sequence analysis revealed no particular homology of the *RVS167* gene to known genes when compared with sequences in standard data bases.

Protein sequence comparison of Rvs167p with data banks revealed several interesting features. The sequence can be split into three clearly separated domains. The C-terminal end of the protein contains a well-conserved SH3 consensus sequence as demonstrated by the alignment made by computer analysis and presented in Fig. 7. This domain is preceded by a sequence of about 130 amino acids rich in glycine (16%), proline (14%), and alanine (28%), called the GPA-rich region (Fig. 8). Charged residues are completely absent in this domain, but it is rich in serine and threonine (18%) residues. The NH_2-terminal part constitutes a third domain presenting important homology with the Rvs161 protein (Fig. 8) and containing two potential cAMP-dependent phosphorylation sites (Fig. 5B).

The SH3 domain was first described as a sequence conserved in the noncatalytic region of the nonreceptor class of protein tyrosine kinases (*src* class). This region of approximately 50 amino acids is present in a very large group of proteins including cytoskeletal elements and signaling proteins. It is believed that the SH3 domain serves as a module that mediates protein-protein interaction and regulates cytoplasmic signaling. In *S. cerevisiae*, the sequence was found in several proteins, such as the actin-binding protein Abp1 (22), Fus1p (78), Cdc25p (10, 12), and Bem1p (15). In some proteins, the SH3 sequence is found in a position similar to that in the Rvs167 protein: the domain is located at the C-terminal end and is preceded by a sequence rich in proline and alanine. This is true for yeast Abp1p (22), for the nonfilamentous myosin I of *Acanthamoeba castellanii* and *Dictyostelium discoideum* (37, 38), and for pp80/85, a recently identified $pp60^{src}$ substrate (83). On the basis of

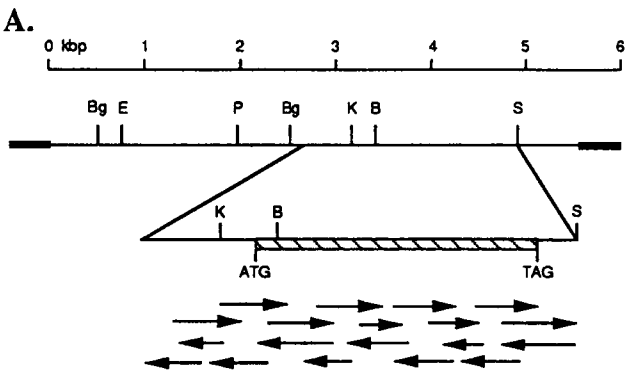

B.

```
AACGTCTTCACTTTCATCTGTAGACATACCTCTATCAAGTTTTGACTTTCCTGTCGCTTGCCTG -327
TACGCTTTTGTTTCTACTGAGAAAAGATACTTTTTGACCATGGACTATAAGTGCACGCTACAGT -263
TGCACATATAAGGTTGTATATAGTTCAAGAAGTTCCTTTCGTATGGAAATTTTGTTATGTATAC -199
CTTCCAGTTGCTATGGTAGTCTACCTGACTAAATTATCAATCCGACCGATGTTCGGATGTTGCG -135
ATAATATTGGTACCGGAAAAAAAAAAAGGAGAGGCTTTGTAGTGTCGATGTTTAACAACCTGTT -71
TTAAGGAATAAAGTAAAGTGAGGCTCACCTGGTCATTTAACACCAAGAATCAAGGAGCCAATAA -7
GTGCAC  ATG AGT TTT AAA GGG TTT ACC AAG GCT GTT AGT AGG GCT CCT  42
        M  S  F  K  G  F  T  K  A  V  S  R  A  P  14
                                          BamHI
CAG TCC TTC CGT CAA AAG TTC AAG ATG GGT GAG CAG ACA GAG GAT CCT  90
 Q  S  F  R  Q  K  F  K  M  G  E  Q  T  E  D  P  30

GTT TAC GAG GAT GCA GAA CGT CGT TTT CAA GAA TTG GAG CAG GAG ACA 138
 V  Y  E  D  A  E  R  R  F  Q  E  L  E  Q  E  T  46

AAA AAA TTA AGT GAG GAA TCG AAG AGA TAC TCG ACT GCG GTG AAT GGA 186
 K  K  L  S  E  E  S  K  R  Y  S  T  A  V  N  G  62

ATG CTG ACA CAC CAA ATT GGA TTT GCC AAA TCC ATG GAG GAA ATT TTC 234
 M  L  T  H  Q  I  G  F  A  K  S  M  E  E  I  F  78

AAA CCT ATC AGT GGT AAA ATG AGT GAC CCT AAC GCT ACC ATA CCA GAG 282
 K  P  I  S  G  K  M  S  D  P  N  A  T  I  P  E  94

GAC AAC CCA CAA GGT ATT GAA GCA AGT GAA CAG TAT AGG GCA ATT GTC 330
 D  N  P  Q  G  I  E  A  S  E  Q  Y  R  A  I  V  110

GCA GAA TTA CAG GAA ACA TTG AAA CCG GAT CTG GCT TTG GTG GAA GAA 378
 A  E  L  Q  E  T  L  K  P  D  L  A  L  V  E  E  126

AAA ATT GTT ACG CCA TGC CAG GAA CTG TTG AAG ATT ATT ACT TAT ATT 426
 K  I  V  T  P  C  Q  E  L  L  K  I  I  T  Y  I  142

CGT AAA ATG GCC ACC AAG AGA AAT CAC AAA AAA TTA GAT TTA GAT AGA 474
 R  K  M  A  T  K  R  N  H  K  K  L  D  L  D  R  158

CAT CTA AAC ACT TAT AAC AAG CAT GAA AAG AAG AAG GAA CCA ACC GCC 522
 H  L  N  T  Y  N  K  H  E  K  K  K  E  P  T  A  174

AAA GAC GAA GAA AGA TTG TAT AAA GCA CAA GCT CAA GTG GAA GTG GCT 570
 K  D  E  E  R  L  Y  K  A  Q  A  Q  V  E  V  A  190

CAA CAA GAA TAT GAT TAC TAT AAC GAC TTG CTA AAG ACT CAA TTA CCA 618
 Q  Q  E  Y  D  Y  Y  N  D  L  L  K  T  Q  L  P  206

ATA CTG TTC AGT TTG GAA GCT GAA TTT GTG AAA CCA TTA TTT GTC TCA 666
 I  L  F  S  L  E  A  E  F  V  K  P  L  F  V  S  222

TTT TAT TTC ATG CAA TTG AAC ATT TTT TAC ACT TTG TAT AAT AGA CTT 714
 F  Y  F  M  Q  L  N  I  F  Y  T  L  Y  N  R  L  238

CAA GAC ATG AAG ATT CCA TAT TTT GAT TTG AAC AGT GAC ATT GTA GAG 762
 Q  D  M  K  I  P  Y  F  D  L  N  S  D  I  V  E  254

TCG TAC ATT GCC AAG AAA GGC AAT GTG GAA GAA CAA ACG GAC GCC TTG 810
 S  Y  I  A  K  K  G  N  V  E  E  Q  T  D  A  L  270

ACT ATT ACA CAC TTT AAA CTC GGT TAC TCT AAG GCA AAA TTG GAG ATG 858
 T  I  T  H  F  K  L  G  Y  S  K  A  K  L  E  M  286

ACC AGA AGG AAG TAT GGT GTA GCA ACC GCC GAA GGC TCA CCC GTC AGT 906
 T  R  R  K  Y  G  V  A  T  A  E  G  S  P  V  S  302

GGC GCA TCA AGC GGT GTC GGA TAT GGT GCT GGG TAT GAT CCA GCA ACT 954
 G  A  S  S  G  V  G  Y  G  A  G  Y  D  P  A  T  318

GCC ACT TCT CCA ACC CCT ACA GGA TAC GGT TAT GGT GCC GCA GCA CCA 1002
 A  T  S  P  T  P  T  G  Y  G  Y  G  A  A  A  P  334

AGT TAC GCC GCT CAA CCT GCT GCC CAG TAT GGT ACT GCT GCC GCC GTT 1050
 S  Y  A  A  Q  P  A  A  Q  Y  G  T  A  A  A  V  350

GGT ACT GCT GCT GCT GTT GGT ACT GCT GCT GGT GCT GCT GCT GGC GCT 1098
 G  T  A  A  A  V  G  T  A  A  G  A  A  A  G  A  366

GTT CCG GGT ACT TAT CCA CAG TAT GCT GCT GCG CAA TCT CCA CCG CTC 1146
 V  P  G  T  Y  P  Q  Y  A  A  A  Q  S  P  P  L  382

ACT GGG CTA GGC TTC CAA CAA TCA CCA CAG CAG CAA CAG GGA CCA CCA 1194
 T  G  L  G  F  Q  Q  S  P  Q  Q  Q  Q  G  P  P  398

CCG GCC TAC TCT AAT CCT CTA ACA TCA CCT GTT GCG GGC ACA CCA GCC 1242
 P  A  Y  S  N  P  L  T  S  P  V  A  G  T  P  A  414

GCG GCC GTA GCG GCA GCT CCT GGC GTT GAA ACT GTT ACC GCA TTG TAT 1290
 A  A  V  A  A  A  P  G  V  E  T  V  T  A  L  Y  430

GAC TAC CAA GCT CAA GCT GCT GGT GAT TTG TCT TTC CCT GCC GGC GCA 1338
 D  Y  Q  A  Q  A  A  G  D  L  S  F  P  A  G  A  446

GTT ATA GAA ATT GTC CAG CGT ACT CCG GAC GTG AAC GAA TGG TGG ACA 1386
 V  I  E  I  V  Q  R  T  P  D  V  N  E  W  W  T  462

GGA AGA TAC AAT GGC CAG CAA GGT GTG TTT CCT GGG AAC TAC GTG CAA 1434
 G  R  Y  N  G  Q  Q  G  V  F  P  G  N  Y  V  Q  478

CTC AAC AAG AAC TAGAGGAGGCCCCTGCATCCCTCTGTATTCATTACCTTCTATTGTGAG 1494
 L  N  K  N                                                    482

ATGTTACCATTACCTTTTTCTTTTATTGTAATGTTTCTTAATTTAAATACTATATAGGGTAATT 1558
CATCCTTCCACCAACAAAGTATCGTTTGAGTCTATCTATTACGGGCATGC                1609
```

FIG. 5. (A) Restriction map of the 5.6-kb insert of the pUKC200-134 plasmid clone containing the *RVS167* gene and sequencing strategy of the complementing DNA fragment. The open reading frame of the RVS167 gene is indicated by the diagonally lined box. The bold lines indicate plasmid DNA. Restriction enzymes are *Bam*HI (B), *Bgl*II (Bg), *Eco*RI (E), *Kpn*I (K), *Pvu*II (P), and *Sph*I (S). No sites were found for *Eco*RV, *Hin*dIII, *Pst*I, *Sal*I, and *Xba*I. (B) DNA sequence of the *RVS167* gene and predicted amino acid sequence of the protein product. The last nucleotide or amino acid of a line is numbered on the right (+1 is assigned to the first base of the initiation codon). The restriction sites *Kpn*I, *Sph*I, and in particular *Bam*HI, used for the disruption, are underlined. Protein sequences underlined with continuous lines correspond to the best-conserved amino acids of the SH3 consensus sequence. Putative cAMP-dependent kinase phosphorylation sites are underlined with dotted lines.

sequence conservation, SH3 and GPA-rich regions from myosin I seem to be the closest relatives of the corresponding Rvs167p regions. However, while the GPA-rich sequences are positively charged in myosin I and negatively charged in Abp1p and pp80/85, the GPA-rich sequence is without any charge in Rvs167p. Different studies suggest that proteins combining GPA-rich and SH3 regions act in actin cortical cytoskeleton organization (22, 61, 84). For example, myosin I seems to allow anchorage and gliding of actin filaments on membranes (3, 61, 84).

Interestingly, the Rvs167 protein shares important homologies with the Rvs161 protein (Fig. 8). As already mentioned, mutants affected in the *RVS161* gene display a phenotype very similar to that of the *rvs167* mutant. Sequence similarity between the two proteins extends throughout all their length, except for the C-terminal region of Rvs167p which covers the GPA-rich and SH3 domains. These domains are absent in Rvs161p. When comparing Rvs167p with the proteins in GenBank, the optimized FASTA score for Rvs161p is 194 (59). This score is the highest for any protein in the data bases, except for myosin IB of *A. castellanii* (optimized FASTA score is 200, but only

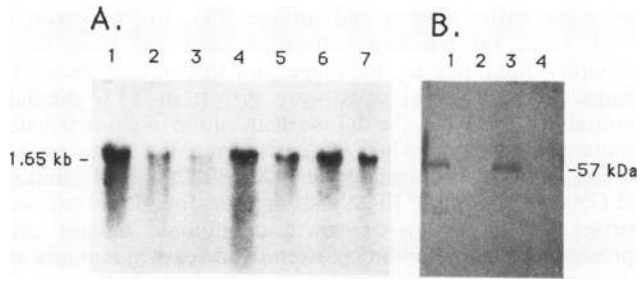

FIG. 6. (A) Northern blot analysis of the *RVS167* mRNA. Total RNA was extracted from the wild-type strain (lanes 1 to 3, 6, and 7) and an *rvs167* mutant strain (lanes 4 and 5). Strains were grown at 26°C in YNB medium except for lane 6 (strain grown in YNBGE containing glycerol and ethanol as carbon sources). The RNA was extracted in the following growth phases and growth conditions: lanes 1, 4, and 6, exponential phase; lanes 2 and 5, transition phase; lane 3, stationary phase; lane 7, heat shock (the RNA was extracted 45 min after the switch from 26 to 39°C). The same quantity of RNA (20 μg) was loaded on each lane. (B) Western blot (immunoblot) analysis of the *RVS167* gene product. Total proteins were extracted from the wild type (lanes 1 and 3), the *rvs167* mutant (lane 2), and the *rvs167::TRP1* disrupted strain (lane 4). The proteins were subjected to SDS-polyacrylamide gel electrophoresis and blotted on a membrane as described in Materials and Methods. The membrane was incubated in 20 ml of TBS buffer with 20 μl of anti-*RVS167* antiserum. The responding band corresponds to a protein with an apparent molecular mass of 57 kDa. No signal was detected in the *rvs167* primary mutant or in the disrupted strain.

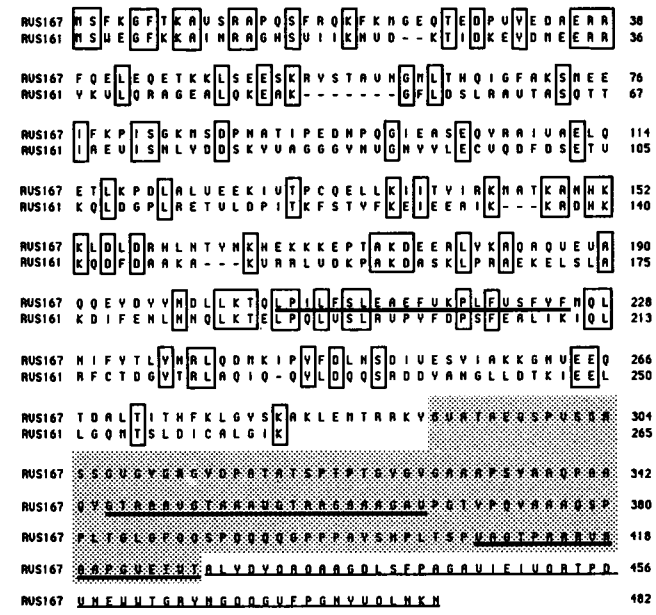

FIG. 8. Structural domains of Rvs167p and comparison of the amino acid sequences of proteins Rvs167 and Rvs161. The last residue of each line is numbered on the right. Only identical amino acid residues are boxed. Gaps, represented by dashes, are introduced in the Rvs161p sequence to optimize the alignment. Homology extends throughout the whole N-terminal domain of Rvs167p. The additional sequences in Rvs167p correspond to the well-defined GPA-rich (grey background) and SH3 (underlined by light lines) domains. Protein stretches probably associated with membrane, determined by the method of Eisenberg et al. (23), are underlined with bold lines.

the GPA-rich and SH3 regions are concerned in this case). A statistical test with the Needleman and Wunsch method (56) comparing the 300 N-terminal amino acids of Rvs167p with Rvs161p and using 100 randomized Rvs161p sequences gives an alignment score of 12.9 standard deviations (SD). The normal score of Rvs161p compared with that of Rvs167p is 25 SD above the mean score. This confirms that the homology between Rvs167 and Rvs161 proteins is statistically significant. The sequence similarity indicates that Rvs161p and Rvs167p are related proteins.

Actin distribution. In *S. cerevisiae*, the actin protein network is involved in a large number of cellular functions, for example, cell polarity, localization of cell wall deposition, and transport of membrane vesicles (2). The actin cytoskeleton therefore seems to organize the morphogenetic development of yeast cells (2), and actin distribution is subjected to characteristic changes during the cell cycle (41). Mutants with nonfunctional actin cytoskeletons present an

A.

```
RVS167   A L Y D Y Q A Q A A G D L S F P A G A V I E I V Q R T P D V N E W W T G R Y N G Q Q G V * * F P G N Y V Q L N K N   Cterm
ABP1     - E - - - D - A E D N E - T - V E N D K - I N I E F V D - * * D - - L - E L E K D G S K G L - - S - - - S - G N   Cterm
P85      - - - - - - - - A G D D E I - - D P D D I - T N I E M I * - D * G - - R - V C K - R Y - L * * - - A - - - E - R Q   Cterm
Myo A.c  - - - - F A - E N P D E - T - N E - - - - T - I N K S N P * * D - - E - E L - - - R - - * * - - A - - - E - I P   .....
Myo D.d  - - - - - D - S S T D E - - - K E - D I - F - - - K * * - N G G - T Q - E L K S G - K G W A * - T - - L - Y -     Cterm
Plc      - - F - - K - - R E D E - T - T K S - I - Q N - E K Q E G * * G - - R - D - H H K K Q I W * - - S - - - E E M V   .....
Fod      - - - - - - - E K S P R E V T M K K - D I - T - I N S - N K * * D - - K V E V - D R - - F W P A A * * - - K K I D   .....
c-Src    - - - - - E S R T E T - - - - K K - E R - Q - - N N - E G * * D - - I A H S I T T G Q T G Y I - S - - - A P S D   .....
c-Abl    - - - - F V R S G D N T - - I T K - E K - R V I G Y N H N G E * - C E A Q T K N G - - W * * V - S - - I T P V N   .....
c-Yes    - - - - - E - R T T D - - - - K G - E R F Q - I N N - E G * * D - - E A - S I A T G K T G Y I - S - - - A P A D   .....
```

B.

```
Seq. con.  A L Y D Y   A       D E L S F     G     I   I V             D W W                   F P S N Y V
RVS167     A L Y D Y Q A Q A A G D L S F P A G A V I E I V Q R T P D V N E W W T G R Y N G Q Q G V F P G N Y V Q L N K
                   :           :   :                 : : : :           :                       :
Myo A.c    - - - - F A - E N P D E - T - N E - - - - T - I N K S N P * * D - - E - E L - - - R - - - - A - - - E - I P
```

FIG. 7. (A) Comparison of the amino acid sequences of the SH3 region of Rvs167p with the SH3 regions of other proteins. Amino acids identical to Rvs167p are represented by dashes. The proteins compared with Rvs167p are as follows: yeast actin binding protein (ABP1) (22), *src* protein kinase substrate pp80/85 (P85) (83), *Acanthamoeba* myosin IB (Myo *A.c*) (37), *Dictyostelium* myosin IB (Myo *D.d*) (38), phospholipase C-γ (Plc) (73), human α-fodrin (Fod) (80), c-Src (76), c-Abl (68), and c-Yes (75). Gaps are represented by asterisks. Cterm indicates that the SH3 region is situated at the C-terminal end of the protein. (B) Alignment of the SH3 domain of Rvs167 with the SH3 consensus sequence and the SH3 domain of myosin I of *A. castellanii*, the closest relative of the corresponding Rvs167p region. The consensus sequence (Seq. con.) corresponds to the amino acids conserved in at least half of the proteins aligned.

abnormal morphology (2, 4, 30, 49, 57). The abnormal cell morphology of the *rvs167* mutant and the presence of the SH3 domain preceded by a GPA-rich sequence, as in Abp1p and myosin I, therefore could indicate possible interaction of the Rvs167 protein with the actin cytoskeleton.

The distribution of actin in *rvs167* mutant cells was examined by fluorescence microscopy using rhodamine-conjugated phalloidin as a fluorescent marker and comparison with distribution in wild-type cells. Analysis was carried out on a large number of cells. The photographs in Fig. 9 show the average phenotype observed in each situation. In exponentially growing cultures in YNB or G1 medium, actin distribution is slightly deregulated in the *rvs167* mutant (Fig. 9). Mother cells during bud emergence contain some more cortical actin spots in mutant than in wild-type cells. Furthermore, in mutant buds, the density of actin spots is rather variable, contrary to what is observed for wild-type cells. However, as in wild-type cells, the distribution varies with the cell cycle and the actin spots are of normal size. Therefore the submembranous actin distribution is still partially regulated, at least in a manner sufficient to assure normal growth and cell morphology in standard conditions.

In starvation conditions or high salt concentrations, the actin cytoskeleton appears to be completely deregulated in the *rvs167* strain (Fig. 9). The phenotype is more intense in NaCl medium. Three hours after addition of NaCl (6% final concentration) to exponentially growing cultures, cortical actin spots are found all around mutant cells, and their distribution seems completely independent from the cell cycle. In addition, spots are frequently of an unusually large size. In growing buds, no concentration of actin can be observed; some buds are even without actin spots at all. Similar observations were made when diploid cells were used (unpublished data).

When NaCl is added to the growth medium, the actin delocalization appears before the morphological changes specific to the *rvs167* phenotype can be observed. Therefore, it seems possible that the actin delocalization causes the abnormal morphology of *rvs167* mutant cells.

Chitin distribution in mutant cells. Cytoskeletal alterations lead sometimes to modified budding patterns and changed chitin deposition (4, 14). We have examined the chitin distribution in the *rvs167* mutants by using calcofluor staining (Fig. 10). This method permits the visualization of chitin deposited in the cell wall and therefore allows the localization of bud scars and the determination of the budding pattern. Yeast cells choose bud sites in two distinct spatial patterns depending on their cell type (21). Haploid cells bud near the site of the previous division (axial budding), whereas diploid cells bud in a bipolar manner either near the site used for the previous division or near the opposite pole.

When chitin distribution and bud scars in haploid cells during the exponential phase of growth and in standard growth conditions were examined, only a slight difference could be observed between wild-type and mutant haploid cells. Mutant cells contain more chitin distributed diffusely over the entire mother cell surface (Fig. 10); however, in both cases the budding pattern is axial and there is no obvious difference in the shape and the size of the chitin rings. When haploid cells were grown in YPD medium containing 3% NaCl, the diffuse distribution of chitin became more pronounced. When we carried out the same experiment on diploid wild-type (X2180-2N) and mutant (LG500-2N and LG510-2N) strains we found, to our surprise, that in standard growth conditions, mutant cells present a random budding pattern. Bud scars in mutants are dispersed over the cell surface, while the wild-type strain presents the normal bipolar budding pattern (Fig. 10). Budding pattern alteration is accompanied by cell shape modifications. Mutant cells show a different shape, with mainly round cells, while the wild-type diploid cells present a regular ovoid shape. This budding defect segregates with the *rvs167-1* mutation.

DISCUSSION

In response to nutrient starvation, the yeast *S. cerevisiae* stops division in the G_1 phase of the cell cycle. Wild-type *S. cerevisiae* accumulates as nonbudding and stress-resistant cells with a homogeneous shape when culture medium becomes exhausted. Then the culture is in stationary phase and cells are in a resting state, referred to as G_0 by analogy with mammalian and avian cells (33). Cells remain viable during prolonged periods of nutritional deprivation.

We selected mutants for loss of viability after nutrient starvation. These mutants respond similarly to carbon and nitrogen starvation, suggesting that the mutations concern a general pathway of the response to nutrient starvation. The criteria used to screen mutants were thought to reveal genes implicated in stationary-phase onset. The strains finally retained, *rvs161* (17) and *rvs167*, show a very similar mutant phenotype specific to nutrient starvation in standard growth conditions. The results described in the present paper concern the *rvs167* mutant.

The mutant analysis revealed two main features. On one hand, the mutant shows a loss of viability and morphological heterogeneity; on the other hand, the budding pattern is altered specifically in diploid cells. Loss of viability and morphological heterogeneity are conditional phenotypes depending on growth conditions and nutrient availability. When growth media are exhausted, cells show a loss of viability and an increased budding ratio accompanied by shape heterogeneity. Further studies showed that mutant cells are sensitive to salt and inhibitors and that they present the same response observed in starvation conditions. These mutant-associated phenotypes indicate that the role of *RVS* genes is not limited to nutrient exhaustion. In any case, the final phenotype of the mutant associates viability loss and morphological heterogeneity.

Sequence analysis showed that the Rvs167 protein contains a SH3 domain preceeded by a GPA-rich region. This global structure is very similar to those found in Abp1 and in

FIG. 9. Actin distribution in wild-type (left) and *rvs167*::*TRP1* (right) cells. Polymerized actin was revealed as described in Materials and Methods by a rhodamine-conjugated phalloidin fluorescent marker. (Upper panels) Actin distribution in log-phase cells grown in YPD medium at 26°C (optical density at 600 nm = 1). Distribution of submembranous actin spots depends on cell cycle position and is regulated in a similar manner in both wild-type and mutant cells. (Middle panel) Actin distribution in cells grown in high salt concentration (6% NaCl) for 3 h. Wild-type cells show normally distributed actin spots, while actin distribution seems to be no longer regulated in mutant cells. The localization of submembranous actin spots is independent from cell cycle position. (Lower panel) Terminal phenotype in starvation conditions of *rvs167*::*TRP1* mutant cells 12 h after stationary-phase entry in G1 medium.

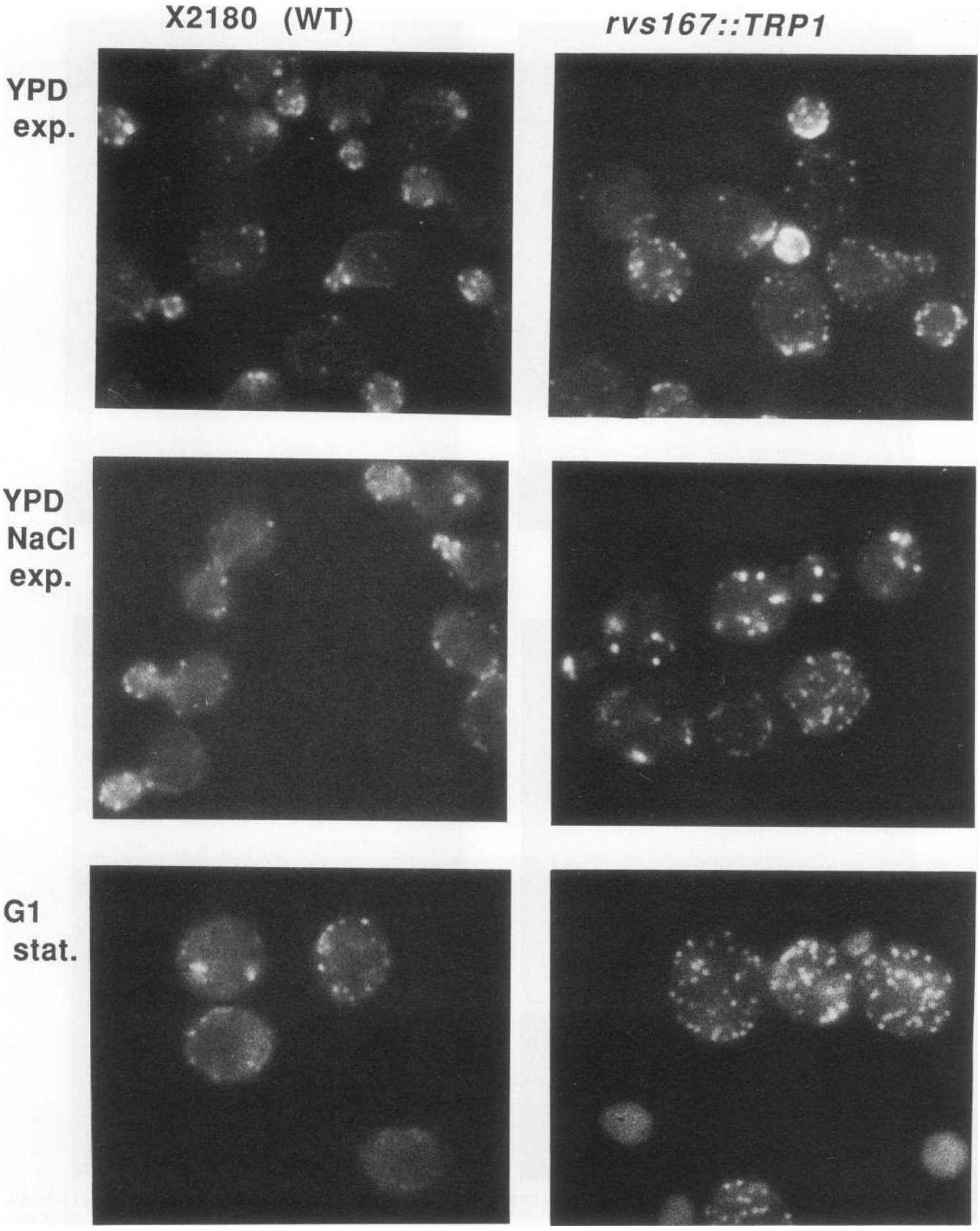
X2180 (WT)
rvs167::TRP1
YPD exp.
YPD NaCl exp.
G1 stat.

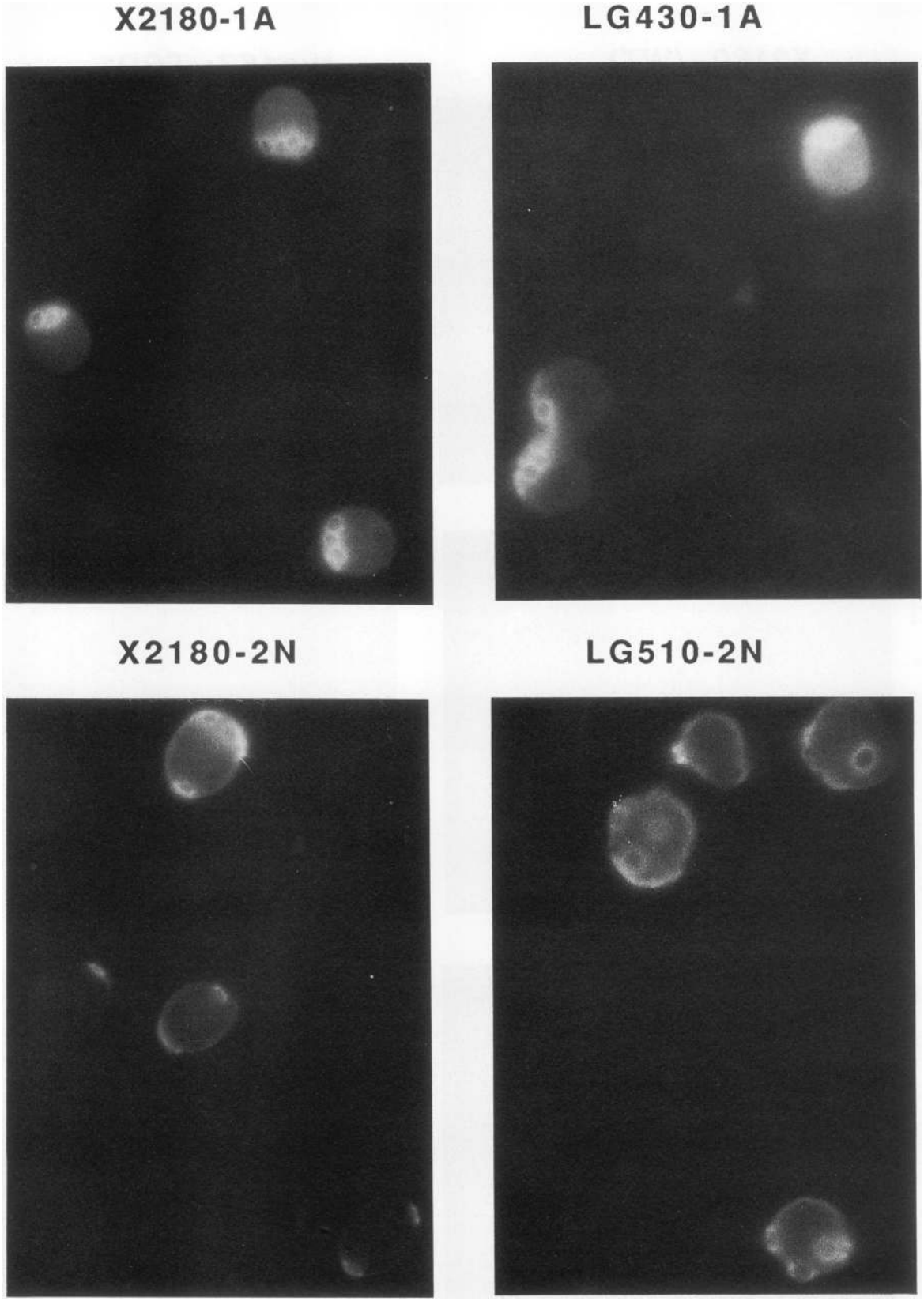

FIG. 10. Chitin and bud scar distribution in wild-type cells (strains X2180-1A and X2180-2N) and *rvs167* mutant cells (strains LG430-1A *rvs167*::*TRP1* and LG510-2N *rvs167*::*TRP1*/*rvs167*::*TRP1*). Cells were stained with the fluorescent dye calcofluor and visualized with epifluorescence microscopy. All strains were grown in YPD medium to mid-exponential phase (optical density at 600 nm = 1) and then treated as described in Materials and Methods. Each photograph presents the average situation observed, except that cells with multiple bud scars were preferentially chosen.

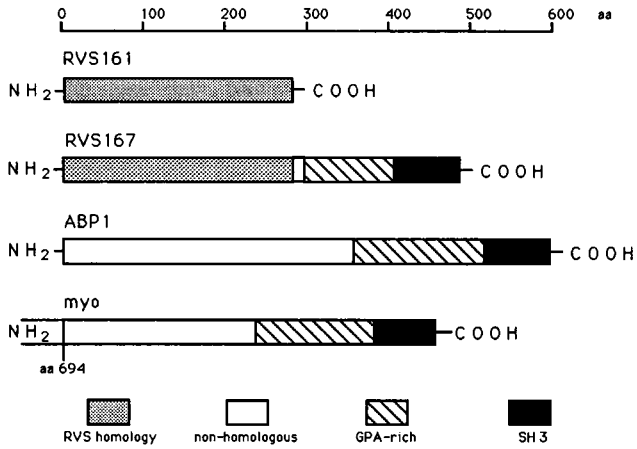

FIG. 11. Comparison of the structural features of Rvs167p with those of Rvs161p (17), Abp1 (22), and the tail of myosin IB of *D. discoideum* (38). The overall structures of Abp1 and the tail of myosin IB are very similar to the Rvs167p structure.

the tail of myosin I known to interact with actin (Fig. 11). The structural similarity of the Rvs167 protein C-terminal part with these proteins led us to examine the membrane-associated cytoskeleton and the cortical actin. Microscopic examination has shown that the actin cytoskeleton is delocalized in the *rvs167* mutants. The severity of the delocalization depends on growth conditions and is more obvious in media containing high salt concentrations. This dramatic delocalization of actin could therefore explain the loss of viability observed in those conditions. Likewise, the increase of budded cells in starved *rvs* mutants may not correspond to defects in cell proliferation control per se. Because of the lack of proper actin distribution, the buds that emerged just before nutrient depletion could be altered in enlargement or cytokinesis, thus increasing the bud ratio in stationary phase. Observation of buds without actin or with variable amounts in starvation conditions favors this hypothesis.

In addition to this phenotype, we found to our surprise that the choice of the budding site is random in *rvs167* diploid mutant cells, whereas it is normally regulated in haploid ones. This alteration suggests an interaction of the *RVS167* gene product with the genes implied in the choice or the formation of the budding site, in which the actin cytoskeleton plays a major role. Two groups of genes are thought to be implicated in these mechanisms. First one group of genes, called *BUD* (12), is directly implied in the choice of the budding site. Indeed, *BUD1/RSR1* (65), *BUD2* (14), or *BUD5* (13) is required for both axial and bipolar patterns; mutants defective in these genes choose bud sites randomly in both haploid and **a**/α cells. *BUD3* and *BUD4* (21) are required only for the axial pattern: mutations in these genes lead to a bipolar budding pattern in haploid cells. Cells carrying those mutations seem not to be otherwise affected, and these genes therefore are thought to define a morphogenetic pathway establishing the budding pattern in haploid and diploid cells. The Budp could be one of a set of proteins that communicates the positional information for normal bud site selection to a second set of proteins that includes Cdc24p (69), Cdc42p and Cdc43p (1), and Bem1p (15). Although at present there are no clear data that address the mechanism by which the proteins function in cellular morphogenesis, three elements are involved in the development of cell polarity: first, the cytoskeleton itself; second, the proteins involved in the choice of the budding site; and third, the proteins implicated in the assembly of the bud site. Interactions between bud site selection and assembly have been observed (13). Likewise, it is clear that bud site selection and assembly are dependent on proper organization of the cytoskeleton. Several arguments suggest that interactions between the budding site and the cytoskeleton are mediated by SH3 domain-containing proteins such as Abp1 (22) and Bem1p (15). But no protein linking the bud site selection determined by *BUD* genes to the cytoskeleton has been identified.

In the *rvs167* mutants, the actin cytoskeleton is delocalized in all types of cells, but the budding pattern is specifically affected in the diploid strain. This situation has not been described in the literature. Thus the choice of bud site in the diploid strain is also specified by the product of the *RVS167* gene which led to the bipolar pattern. This indicates that Rvs167p interacts with proteins and perhaps with the Bud proteins that recognize the landmark in **a**/α cells. We imagine that Rvs167p does not intervene in budding site selection in haploid cells; the Bud proteins have to recognize other cellular components to lead to the axial pattern. Then, according to the model proposed by Chant and Herskowitz (14), Rvs167p cannot be in the direct pathway composed of Bud proteins but in a branch of this pathway interacting with the Bud1p, Bud2p, and Bud5p in diploid cells only. However, there are notable differences between the BUD genes and the *RVS167* gene; unlike mutations in the BUD genes, the mutation *rvs167-1* is very pleiotropic and leads in particular to morphologic abnormality with altered actin cytoskeleton in haploid and diploid cells. These properties suggest that Rvs167p might alter the link of the cytoskeleton to morphogenetic determinants on the cell surface and to budding site in diploid cells.

This hypothesis alone cannot explain the conditional loss of viability and the morphological heterogeneity observed only in starvation and in unfavorable growth conditions. This conditional phenotype suggests that the Rvs167 protein should be involved in a cellular adaptation to starvation and unfavorable growth conditions. Many responses to nutrient limitation in *S. cerevisiae* seem to be regulated via the cAMP and its related protein phosphorylation system (28, 77). Two putative cAMP-dependent phosphorylation sites exist in the Rvs167 protein. Interestingly, some elements of this pathway have recently been shown to interact with the cytoskeleton via the bifunctional adenylate cyclase-associated CAP protein (79). While the N-terminal part of this protein seems to interact with RAS and adenylate cyclase (25, 26), mutations in the C-terminal part lead to phenotypes which, in some respects, are very similar to the *rvs167* phenotype, including sensitivity to starvation and a random budding pattern (27); in addition, cap mutants are also sensitive to 3-amino-1,2,4-triazole. The authors attribute to this protein a function in the regulation of the cytoskeleton in response to growth signals (79). Considering this mutant phenotype, it is attractive to speculate that the Rvs167 protein could be an effector of this pathway acting in association with some elements of the cAMP pathway. This second hypothesis permits us to link the delocalization of the cytoskeleton with the loss of viability observed in defined conditions; thus, Rvs167 protein might be implicated in cytoskeletal reorganization in response to particular growth conditions.

The two hypotheses presented in this discussion are not mutually exclusive. Indeed, the two mentioned mechanisms

could be associated in some cellular adaptations to starvation, for example, pseudohyphal differentiation (29).

The *rvs161* mutants (17) present the same phenotype as *rvs167* mutants and therefore should be implicated in similar functions. Interestingly, the two proteins Rvs161 and Rvs167 reveal themselves as somewhat related proteins. Important homology is observed throughout the whole Rvs161 protein sequence of 265 amino acids with the 300-amino-acid N-terminal domain of the Rvs167 protein. The additional sequences in Rvs167p are the clearly defined SH3 and GPA-rich domains. Although Rvs161p does not possess this region, mutations in RVS161 lead also to the same defects in actin distribution (unpublished data).

Several arguments suggest that both *RVS* genes act in the same or at least in very similar mechanisms. Besides the already-mentioned fact that the two *rvs* single mutants and the *rvs161 rvs167* double mutant have indistinguishable phenotypes in respect to all the conditions examined and in particular the budding pattern, suppressor genes of the *rvs161* phenotype identified in our laboratory were revealed to suppress also the *rvs167* phenotype (19). This result reinforces the idea that the two genes act in the same mechanism. Sequence similarity between Rvs161 and Rvs167 proteins, therefore, seems physiologically significant and should facilitate functional exploration of protein regions. Nevertheless, no cross-complementation between the two *RVS* genes could be observed, even when using multicopy vectors. So, even if Rvs161 and Rvs167 proteins execute similar functions and act in the same mechanism, they must play distinguishable roles. Nevertheless, these proteins could be associated in one complex, thus explaining the similarity of all phenotypes shown by the single and double mutants. Such a situation was described for subunits a and b of the capping protein encoded by the *CAP1* and *CAP2* genes in *S. cerevisiae* (5).

ACKNOWLEDGMENTS

We thank M. F. Peypouquet for expert technical assistance and C. Suire for help with fluorescence microscopy.

This work was supported by grants from the CNRS. F. Bauer was supported by the MRT (Ministère de la Recherche et de la Technologie).

REFERENCES

1. **Adams, A. E. M., D. I. Johnson, R. M. Longnecker, B. F. Sloat, and J. R. Pringle.** 1990. CDC42 and CDC43, two additional genes involved in budding and the establishment of cell polarity in the yeast *S. cerevisiae*. J. Cell Biol. **111**:131–142.
2. **Adams, A. E. M., and J. R. Pringle.** 1984. Relationship of actin and tubulin distribution to bud growth in wild type and morphogenetic-mutant *Saccharomyces cerevisiae*. J. Cell Biol. **98**:934–945.
3. **Adams, R. J., and T. D. Pollard.** 1990. Binding of myosin I to membrane lipids. Nature (London) **340**:565–568.
4. **Amatruda, J. F., J. F. Cannon, K. Tatchell, C. Hug, and J. A. Cooper.** 1990. Disruption of the actin cytoskeleton in yeast capping protein mutants. Nature (London) **344**:352–354.
5. **Amatruda, J. F., D. J. Gattermeir, T. Karpova, and J. A. Cooper.** 1992. Effects of null mutations and overexpression of capping protein on morphogenesis, actin distribution and polarized secretion in yeast. J. Cell Biol. **119**:1151–1162.
6. **Becker, J. U.** 1978. A method for glycogen determination in whole yeast cells. Anal. Biochem. **86**:56–64.
7. **Birnboim, H. C., and T. Doly.** 1979. A rapid alkaline extraction procedure for screening recombinant plasmid DNA. Nucleic Acids Res. **7**:1513–1523.
8. **Bonneu, M., M. Crouzet, M. Urdaci, and M. Aigle.** 1991. Direct detection of yeast mutants with reduced viability on plates by erythrosine B staining. Anal. Biochem. **193**:225–230.
9. **Boucherie, H.** 1985. Protein synthesis during transition and stationary phases under glucose limitation in *Saccharomyces cerevisiae*. J. Bacteriol. **161**:385–392.
10. **Broek, D., T. Toda, T. Michaeli, L. Levin, C. Birchmeier, M. Zoller, S. Powers, and M. Wigler.** 1987. The *S. cerevisiae CDC25* gene product regulates the RAS/adenylate cyclase pathway. Cell **48**:789–799.
11. **Cameron, S., L. Lenny, M. Zoller, and M. Wigler.** 1988. cAMP-independent control of sporulation, glycogen metabolism, and heat shock resistance in *S. cerevisiae*. Cell **53**:555–566.
12. **Camonis, J. H., M. Kalékine, B. Gondré, H. Garreau, E. Boy-Marcotte, and M. Jacquet.** 1986. Characterization, cloning and sequence analysis of the *CDC25* gene which controls the cyclic AMP level of *Saccharomyces cerevisiae*. EMBO J. **5**:375–380.
13. **Chant, J., K. Corrado, J. R. Pringle, and I. Herskowitz.** 1991. Yeast *BUD5*, encoding a putative GDP-GTP exchange factor, is necessary for bud site selection and interacts with bud formation gene *BEM1*. Cell **65**:1213–1224.
14. **Chant, J., and I. Herskowitz.** 1991. Genetic control of bud site selection in yeast by a set of gene products that constitute a morphogenetic pathway. Cell **65**:1203–1212.
15. **Chenevert, J., K. Corrado, A. Bender, J. R. Pringle, and I. Herskowitz.** 1992. A yeast gene (*BEM1*) necessary for cell polarization whose product contains two SH3 domains. Nature (London) **356**:77–79.
16. **Cross, F. R.** 1988. *DAF1*, a mutant gene affecting size control, pheromone arrest, and cell cycle kinetics of *Saccharomyces cerevisiae*. Mol. Cell. Biol. **8**:4675–4684.
17. **Crouzet, M., M. Urdaci, L. Dulau, and M. Aigle.** 1991. Yeast mutant affected for viability upon nutrient starvation: characterization and cloning of the *RVS161* gene. Yeast **7**:727–743.
18. **Dayhoff, M. O.** 1978. Atlas of protein sequence and structure, vol. 3, p. 1–8. National Biomedical Research Foundation, Washington, D.C.
19. **Desfarges, L., P. Durrens, H. Juguelin, C. Cassagne, M. Bonneu, and M. Aigle.** 1993. Yeast mutants affected in viability upon starvation have a modified phospholipid composition. Yeast **9**:267–277.
20. **Deutch, C. E., and J. M. Parry.** 1974. Spheroplast formation in yeast during the transition from exponential phase to stationary phase. J. Gen. Microbiol. **80**:259–266.
21. **Drubin, D. G.** 1991. Development of cell polarity in budding yeast. Cell **65**:1093–1095.
22. **Drubin, D. G., J. Mulholland, Z. Zhu, and D. Botstein.** 1990. Homology of a yeast actin-binding protein to signal transduction proteins and myosin I. Nature (London) **343**:288–290.
23. **Eisenberg, D., E. Schwarz, M. Komaromy, and R. Wall.** 1984. Analysis of membrane and surface protein sequences with the hydrophobic moment plot. J. Mol. Biol. **179**:125–142.
24. **Falco, S. C., Y. Li, J. R. Broach, and D. Botstein.** 1982. Genetic properties of chromosomally integrated 2μ plasmid DNA in yeast. Cell **29**:573–584.
25. **Fedor-Chaiken, M., R. J. Deschenes, and J. R. Broach.** 1990. *SRV2*, a gene required for *RAS* activation of adenylate cyclase in yeast. Cell **61**:329–340.
26. **Field, J., A. Vojtek, R. Ballester, G. Bolger, J. Colicelli, K. Ferguson, J. Gerst, T. Kataoka, T. Michaeli, S. Powers, M. Riggs, L. Rodgers, I. Wieland, B. Wheland, and M. Wigler.** 1990. Cloning and characterization of *CAP*, the *S. cerevisiae* gene encoding the 70kd adenylyl cyclase-associated protein. Cell **61**:319–327.
27. **Gerst, J. E., K. Ferguson, A. Vojtek, M. Wigler, and J. Field.** 1991. *CAP* is a bifunctional component of the *Saccharomyces cerevisiae* adenylyl cyclase complex. Mol. Cell. Biol. **11**:1248–1257.
28. **Gibbs, J. B., and M. S. Marshall.** 1989. The *ras* oncogene—an important regulatory element in lower eucaryotic organisms. Microbiol. Rev. **53**:171–185.
29. **Gimeno, C. J., P. O. Ljungdahl, C. A. Styles, and G. R. Fink.** 1992. Unipolar cell divisions in the yeast *S. cerevisiae* lead to

filamentous growth: regulation by starvation and *RAS*. Cell **68**:1077–1090.
30. **Haarer, B. K., S. H. Lillie, A. E. M. Adams, V. Magdolen, W. Bandlow, and S. S. Brown.** 1990. Purification of profilin from *Saccharomyces cerevisiae* and analysis of profilin-deficient cells. J. Cell Biol. **110**:105–114.
31. **Hoffmann, C. S., and F. Winston.** 1987. A ten minute DNA preparation from yeast efficiently releases autonomous plasmids for transformation of *Escherichia coli*. Gene **57**:267–272.
32. **Iida, H., and I. Yahara.** 1984. Specific early G1 blocks accompanied with stringent response in *Saccharomyces cerevisiae* lead to growth arrest in resting state similar to the G0 of higher eucaryotes. J. Cell Biol. **98**:1185–1193.
33. **Iida, H., and I. Yahara.** 1984. Durable synthesis of high molecular weight heat shock proteins in G0 cells of the yeast and other eucaryotes. J. Cell Biol. **99**:199–207.
34. **Ito, H., Y. Fukuda, K. Murata, and A. Kimura.** 1983. Transformation of intact yeast cells treated with alkali cations. J. Bacteriol. **153**:163–168.
35. **Jacquet, M., and J. Camonis.** 1985. Contrôle du cycle de division cellulaire et de sporulation chez *S. cerevisiae*. Biochimie **67**:35–43.
36. **Johnston, G. C., J. R. Pringle, and L. H. Hartwell.** 1977. Coordination of growth with cell division in the yeast *Saccharomyces cerevisiae*. Exp. Cell Res. **105**:79–98.
37. **Jung, G., E. D. Korn, and J. A. Hammer III.** 1987. The heavy chain of *Acanthamoeba* myosin IB is a fusion of myosin-like and non-myosin-like sequences. Proc. Natl. Acad. Sci. USA **84**:6720–6724.
38. **Jung, G., C. L. Saxe III, A. R. Kimmel, and J. A. Hammer III.** 1989. *Dictyostelium discoideum* contains a gene encoding a myosin I heavy chain. Proc. Natl. Acad. Sci. USA **86**:6186–6190.
39. **Kataoka, T., S. Powers, C. McGill, O. Fasano, J. Strathern, J. Broach, and M. Wigler.** 1984. Genetic analysis of yeast *RAS1* and *RAS2* genes. Cell **37**:437–445.
40. **Kieny, M. P., R. Lathe, and J. P. Lecocq.** 1983. New versatile cloning and sequencing vectors based on bacteriophage M13. Gene **26**:91–99.
41. **Kilmartin, J. V., and A. E. M. Adams.** 1984. Structural rearrangements of tubulin and actin during the cell cycle of the yeast *Saccharomyces*. J. Cell Biol. **98**:922–933.
42. **Koch, C. A., D. Anderson, M. F. Moran, C. Ellis, and T. Pawson.** 1991. SH2 and SH3 domains: elements that control interactions of cytoplasmic signalling proteins. Science **252**:668–674.
43. **Koerner, T. J., J. E. Hill, A. M. Myers, and A. Tzagoloff.** 1989. High-expression vectors with multiple cloning sites for construction of *trpE*-fusion genes: pATH vectors. Methods Enzymol. **194**:477–490.
44. **Kraft, R., J. Tardiff, K. S. Krauter, and L. A. Leinwand.** 1988. Using miniprep plasmid DNA for sequencing double stranded templates with Sequenase. BioTechniques **6**:544–549.
45. **Kurjan, J.** 1992. Pheromone response in yeast. Annu. Rev. Biochem. **61**:1097–1129.
46. **Laemmli, U. K.** 1970. Cleavage of structural proteins during the assembly of the head of bacteriophage T4. Nature (London) **227**:680–685.
47. **Lehto, V.-P., V. M. Wasenius, P. Salvén, and M. Saraste.** 1988. Transforming and membrane proteins. Nature (London) **334**: 388. (Letter.)
48. **Lillie, S. H., and J. R. Pringle.** 1980. Reverse carbohydrate metabolism in *Saccharomyces cerevisiae*: responses to nutrient limitation. J. Bacteriol. **143**:1384–1394.
49. **Liu, H., and A. Bretscher.** 1989. Disruption of the single tropomyosin gene in yeast results in the disappearance of actin cables from the cytoskeleton. Cell **57**:233–242.
50. **Matsumoto, K., I. Uno, and T. Ishikawa.** 1985. Genetic analysis of the role of cAMP in yeast. Yeast **1**:15–24.
51. **Matsumoto, K., I. Uno, Y. Oshima, and T. Ishikawa.** 1982. Isolation and characterization of yeast mutants deficient in adenylate cyclase and cAMP-dependent protein kinase. Proc. Natl. Acad. Sci. USA **79**:2355–2364.
52. **McIntosh, E. M., and R. H. Haynes.** 1986. Sequence and expression of the dCMP deaminase gene (*DCD1*) of *Saccharomyces cerevisiae*. Mol. Cell. Biol. **6**:1711–1721.
53. **Miller, J. H.** 1972. Experiments in molecular genetics, p. 431–435. Cold Spring Harbor Laboratory Press, Cold Spring Harbor, N.Y.
54. **Mortimer, R. K., and D. C. Hawthorne.** 1969. Yeast genetics, p. 385–460. *In* A. H. Rose and J. S. Harrison (ed.), The yeasts, vol. 1. Academic Press, Inc., New York.
55. **Myers, E. W., and W. Miller.** 1988. A software tool for finding locally optimal alignments in protein and nucleic acid sequences. Comput. Appl. Biosci. **4**:11–17.
56. **Needleman, S. H., and C. D. Wunsch.** 1970. A general method applicable to the search for similarities in the amino acid sequence of two proteins. J. Mol. Biol. **48**:443–453.
57. **Novick, P., B. C. Osmond, and D. Botstein.** 1989. Suppressors of yeast actin mutations. Genetics **121**:659–674.
58. **Okayama, H., and P. Berg.** 1982. High-efficiency cloning of full-length cDNA. Mol. Cell. Biol. **2**:161–170.
59. **Pearson, W. R., and D. J. Lipman.** 1988. Improved tools for biological sequence comparison. Proc. Natl. Acad. Sci. USA **85**:2444–2448.
60. **Plesset, J., J. R. Ludwig, B. S. Cox, and C. S. McLaughlin.** 1987. Effect of cell cycle position on thermotolerance in *Saccharomyces cerevisiae*. J. Bacteriol. **169**:779–784.
61. **Pollard, T., S. K. Doberstein, and H. T. Zot.** 1991. Myosin I. Annu. Rev. Physiol. **53**:653–681.
62. **Pringle, J. R.** 1991. Staining of bud scars and other cell wall chitin with calcofluor. Methods Enzymol. **194**:732–735.
63. **Rodaway, A. R., M. J. E. Sternberg, and D. L. Bentley.** 1989. Similarity in membrane proteins. Nature (London) **342**:624. (Letter.)
64. **Rothstein, R. J.** 1983. One step gene disruption in yeast. Methods Enzymol. **101**:202–211.
65. **Ruggieri, R., A. Bender, Y. Matsui, S. Powers, Y. Takai, J. R. Pringle, and K. Matsumoto.** 1992. *RSR1*, a *ras*-like gene homologous to *Krev*-1 (*smg21A*/*rap1A*): role in the development of cell polarity and interactions with the Ras pathway in *Saccharomyces cerevisiae*. Mol. Cell. Biol. **12**:758–766.
66. **Sanger, F., S. Nicklen, and A. R. Coulson.** 1977. DNA sequencing with chain-terminating inhibitors. Proc. Natl. Acad. Sci. USA **74**:5463–5467.
67. **Sherman, F., G. R. Fink, and J. B. Hicks.** 1986. Methods in yeast genetics. Cold Spring Harbor Laboratory Press, Cold Spring Harbor, N.Y.
68. **Shtivelman, E., B. Lifshitz, R. Gale, B. Roe, and E. Canaani.** 1986. Alternative splicing of RNAs transcribed from the human *abl* gene and from the *bcr-abl* fused gene. Cell **47**:277–284.
69. **Sloat, B. F., A. Adams, and J. R. Pringle.** 1981. Roles of the *CDC24* gene product in cellular morphogenesis during the *Saccharomyces cerevisiae* cell cycle. J. Cell Biol. **89**:395–405.
70. **Smith, D. B., and K. S. Johnson.** 1988. Single step purification of polypeptides expressed in *Escherichia coli* as fusions with glutathione S-transferase. Gene **67**:31–40.
71. **Southern, E. M.** 1975. Detection of specific sequences among DNA fragments separated by gel electrophoresis. J. Mol. Biol. **98**:503–517.
72. **Sprague, G. F., Jr.** 1991. Signal transduction in yeast mating: receptors, transcription factors, and the kinase connection. Trends Genet. **7**:393–398.
73. **Stahl, M. L., C. R. Ferenz, K. L. Kelleher, R. W. Kriz, and J. L. Knopf.** 1988. Sequence similarity of phospholipase C with the noncatalytic region of *src*. Nature (London) **332**:269–272.
74. **Sudbery, P. E., A. R. Goodey, and B. L. A. Carter.** 1980. Genes which control cell proliferation in the yeast *Saccharomyces cerevisiae*. Nature (London) **288**:401–404.
75. **Sukegawa, J., K. Semba, Y. Yamanashi, M. Nishizawa, N. Miyajima, T. Yamamoto, and K. Toyoshima.** 1987. Characterization of cDNA clones for the human c-*yes* gene. Mol. Cell. Biol. **7**:41–47.
76. **Takeya, T., and H. Hanafusa.** 1983. Structure and sequence of the cellular gene homologous to the RSV *src* gene and the

mechanism for generating the transforming virus. Cell **32:**881–890.

77. **Thevelein, J. M.** 1991. Fermentable sugars and intracellular acidification as specific activators of the RAS-adenylate cyclase signalling pathway in yeast: the relationship to nutrient induced cell cycle control. Mol. Microbiol. **5:**1301–1307.
78. **Trueheart, J., J. D. Boeke, and G. R. Fink.** 1987. Two genes required for cell fusion during yeast conjugation: evidence for a pheromone-induced surface protein. Mol. Cell. Biol. **7:**2316–2328.
79. **Vojtek, A., B. Haarer, J. Fields, J. Gerst, T. D. Pollard, S. Brown, and M. Wigler.** 1991. Evidence for a functional link between profilin and CAP in the yeast *S. cerevisiae*. Cell **66:**497–505.
80. **Wasenius, V. M., M. Saraste, P. Salven, M. Eramaa, L. Holm, and V. P. Letho.** 1989. Primary structure of the brain "Alpha" spectrin. J. Cell Biol. **108:**79–83.
81. **Wheals, A. E.** 1987. Biology of the cell cycle in yeasts, p. 283–390. *In* A. Rose and J. Harrison (ed.), Biology of yeasts, vol. 1. Academic Press, New York.
82. **Wolfner, M., D. Yep, F. Messenguy, and G. Fink.** 1975. Integration of amino acid biosynthesis into the cell cycle of *Saccharomyces cerevisiae*. J. Mol. Biol. **96:**273–290.
83. **Wu, H., A. B. Reynolds, S. B. Kanner, R. R. Vines, and J. T. Parsons.** 1991. Identification and characterization of a novel cytoskeleton-associated $pp60^{src}$ substrate. Mol. Cell. Biol. **11:**5113–5124.
84. **Zot, H. G., S. K. Doberstein, and T. D. Pollard.** 1992. Myosin I moves actin filaments on a phospholipid substrate: implications for membrane targeting. J. Cell Biol. **116:**367–376.